Received: 24 February 2017 | Revised: 30 November 2017 | Accepted: 6 December 2017

DOI: 10.1111/ter.12319

PAPER

WILEY Terra Nova

Dating palaeo-seismic faulting in the Taiwan Mountain Belt

Chih-Tung Chen[1,2] | Chieh-Yu Wu[2] | Ching-Hua Lo[2] | Hao-Tsu Chu[3] | Tzen-Fu Yui[4]

[1]Department of Earth Sciences, National Central University, Zhongli, Taiwan, R.O.C.

[2]Department of Geosciences, National Taiwan University, Taipei, Taiwan, R.O.C.

[3]Institute of Applied Geology, National Central University, Zhongli, Taiwan, R.O.C.

[4]Institute of Earth Sciences, Academia Sinica, Taipei, Taiwan, R.O.C.

Correspondence
Chih-Tung Chen, Department of Earth Sciences, National Central University, Zhongli, Taiwan, R.O.C.
Email: chihtung@ncu.edu.tw; kthomasch@gmail.com

Funding information
Ministry of Science and Technology, Taiwan, R.O.C., Grant/Award Number: 106-2119-M-008-023, 102-2116-M-002-027-MY3, 105-2811-M-002-123, 106-2116-M-002-017; National Central University

Abstract

In-situ $^{40}Ar/^{39}Ar$ laser microprobe dating was carried out on the Hoping pseudotachylite from a mylonite-fault zone in the metamorphosed basement complex of the active Taiwan Mountain Belt to determine the timing of the responsible earthquake(s). The dating results, distributed from 3.2 to 1.6 Ma with errors ranging from 0.2 to 1.1 Ma, were derived from a combination of two Ar isotopic system end-members with inverse isochron ages of 1.55 ± 0.05 and 2.87 ± 0.07 Ma, respectively. Petrographical observations reveal fault melt containing ultracataclasites, therefore the older inverse isochron end-member may be attributed to the relic wall rock Ar isotopic system contained in micro-breccia. Without significant Ar loss expected, the ~1.6 Ma for the young end-member defines the exact time of the pseudotachylite formation. Seismic faulting therefore occurred during basement rock exhumation in the Taiwanese hinterland.

1 | INTRODUCTION

Pseudotachylites are the only undisputed geological records of earthquake fault rupture (Cowan, 1999), as they represent the frozen products of its characteristic high-rate frictional slip (Di Toro, Nielsen, & Pennacchioni, 2005). The non-equilibrated melt phase, often contemporaneous with cataclasis, preserves clues to the dynamic earthquake processes which are unavailable from indirect seismological observations (Di Toro et al., 2005), yet crucial for insights into seismo-tectonics of both present-day and past tectonic settings (e.g. Sherlock, Strachan, & Jones, 2009). However, outcrops containing pseudotachylites are extremely rare and concentrated in crystalline rocks (Sibson & Toy, 2007), limiting our knowledge of earthquake processes at seismogenic depths. The island of Taiwan, a site of ongoing convergence between the Eurasian and Philippine Sea plates and associated mountain building (Suppe, 1981), offers a unique opportunity to link modern-day seismic activities with rock records of earthquakes because of ultra-fast exhumation in the Central Range (Fuller, Willett, Fisher, & Lu, 2006; Hsu et al., 2016). Rocks in the Central Range were metamorphosed to greenschist up to lower-amphibolite facies during the Neogene orogeny (Beyssac et al., 2007; Chen, Chan, Lu, Simoes, & Beyssac, 2011), thereby exposing materials recently deformed in the seismogenic section of the crust (Chan, Okamoto, Yui, Iizuka, & Chu, 2005; Chu, Hwang, Shen, & Yui, 2012).

Although Taiwan is seismically extremely active (Wu, Chang, Zhao, Teng, & Nakamura, 2008), findings of fault pseudotachylites have been recent and limited. They were first described in the drill cores taken from the causative fault of the 1999 Chi-Chi Earthquake in the Western Foothills (Figure 1a; Boullier, Yeh, Boutareaud, Song, & Tsai, 2009). While seismological constraints for the genesis of the Chelungpu pseudotachylites are comprehensive, the shallow depths of their recovery (< 1.5 km) were probably not representative of hypocentral conditions. A recent discovery in the metamorphic hinterland in eastern Central Range, the Hoping pseudotachylite, (Chu et al., 2012; Figure 1), provides a better candidate for studying seismogenic-depth earthquake rupture processes. The Hoping pseudotachylite was developed within the upper-greenschist Tachoshui granitic gneiss along a ductile reverse shear zone (Chiao, 1991; Wang, Lin, & Lo, 1998) before being exhumed from depths of over 5 km (Chu et al., 2012). Studies of the structure (Chu et al., 2012; Ferre et al., 2016a; Korren, Ferre, Yeh, Chou, & Chu, 2017), mineralogy and geochemistry (Chu et al., 2012; Kuo, 2016), and magnetic properties (Ferre et al., 2016b; Kuo, 2016) provide information on the dynamic processes involved in its formation, presumably a seismic event of Mw > 6 (Korren et al., 2017). Nonetheless, key

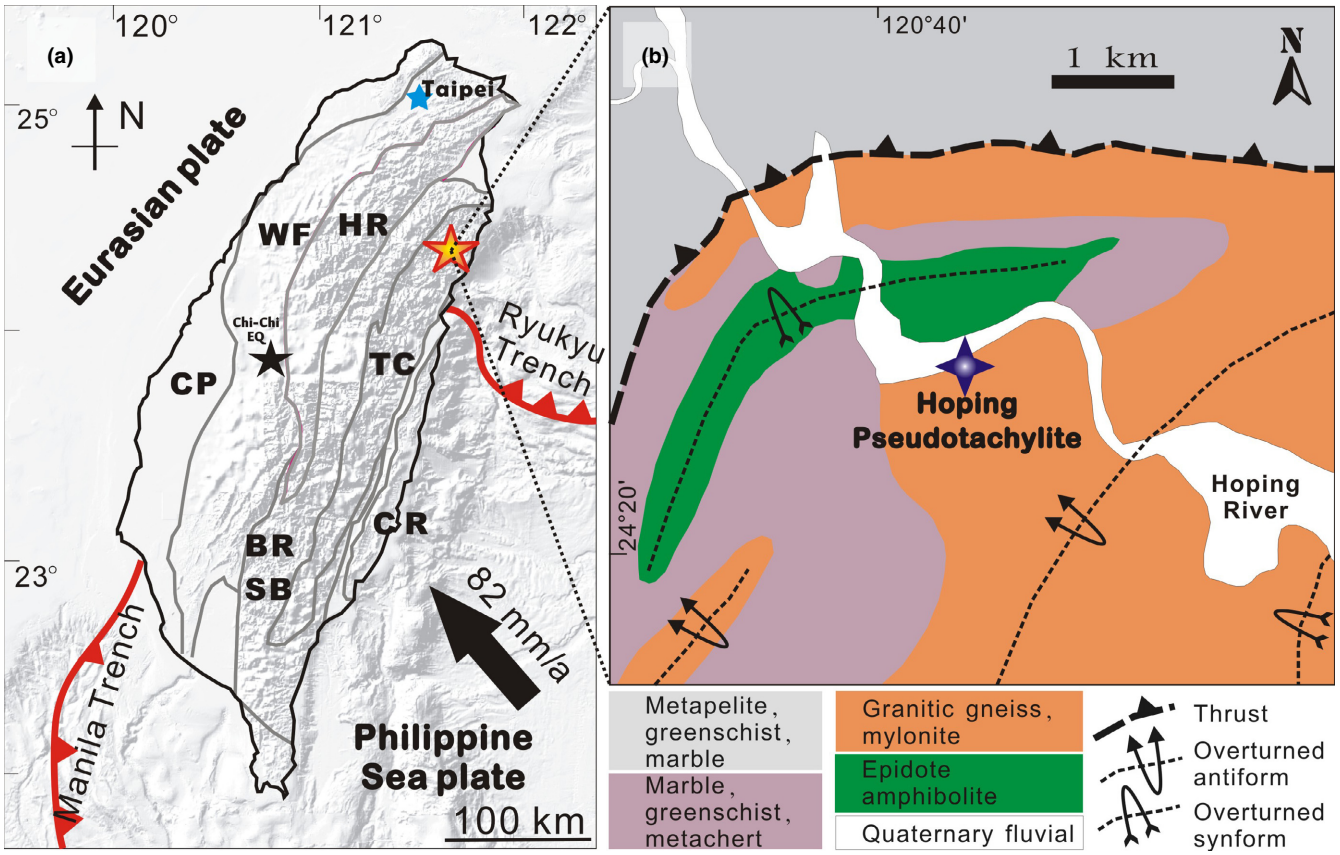

FIGURE 1 (a) Tectonic outline of Taiwan: CR, Coastal Range; TC, Tananao Complex; BRSB, Backbone Range Slate Belt; HR, Hsuehshan Range; WF, Western Foothills; CP, Coastal Plain. Locations of the Hoping pseudotachylite and the 1999 Chi-Chi Earthquake are marked with red and black stars, respectively. (b) Simplified geologic map of the Hoping Area. The pseudotachylite locality is marked by blue star and is on mylonitic gneiss along the gneiss-marble unit boundary shear zone [Colour figure can be viewed at wileyonlinelibrary.com]

information on the timing of the paleo-earthquake remains unknown, thus making it difficult to place the pseudotachylite-generating event in the seismotectonic context of the Taiwan orogen.

Age determination of pseudotachylites is usually confined to the $^{40}Ar/^{39}Ar$ dating method since biotite and amphibole, both K-bearing minerals, are usually first molten due to relatively low melting temperature and weak mechanical strength (Sherlock et al., 2009). The near-instantaneous formation of pseudotachylite through earthquake frictional heating followed by immediate quench solidification potentially resets the K-Ar isotopic system, and such a heterogeneous mixture of melt and cataclastic fragments is best analyzed using a laser microprobe (Kelley, Reddy, & Maddock, 1994; Sherlock et al., 2009). In this work, *in-situ* $^{40}Ar/^{39}Ar$ laser microprobe dating has been carried out in conjunction with structural-petrographic observations on the Hoping pseudotachylite providing firm temporal constraints on its formation.

1.1 | Geological setting and the pseudotachylite

The Taiwan mountain belt results from oblique collision between the Chinese continental margin and the Luzon Arc (Suppe, 1981) starting ~6.5 Ma (onset of foreland deposition; Lin, Watts, & Hesselbo, 2003) till the present (Shyu, Sieh, & Chen, 2005). There are 4 general physiographic units in the Taiwan mountain belt (Figure 1a): (1) the foreland basin of the Coastal Plain, (2) the fold-thrust belt of the Western Foothills and the Slate Belt (Chen et al., 2011), (3) the exhumed Tananao metamorphic complex in eastern Central Range, and 4) the accreted arc of the Coastal Range. The Hoping pseudotachylite is found in the Tailuko Belt of the Tananao Complex, which is the metamorphosed pre-Tertiary basement of Chinese continental margin affinity. It consists of metasediment, meta-ophiolitic rocks and metamorphosed Mesozoic granitoids (Yui et al., 2009). The Tailuko Belt was subjected to greenschist and, locally, lower-amphibolite facies metamorphism during the Neogene collisional orogeny (Beyssac et al., 2007; Lo & Onstott, 1995), when it was tectonically-loaded through underthrusting to mid-crustal depths (e.g. Malavieille, 2010) and acquired thrust shear contacts among the rock units (Chiao, 1991; Suppe, 1981). The collision matures in central-northern Taiwan, where the Hoping area is located, due to the distinct spatial-temporal relationship during the orogeny rendered by the oblique convergence setting (Suppe, 1981), thus allowing exposure of the basement rocks, once deep-seated within the orogenic pile, through rapid exhumation (Fuller et al., 2006).

The Hoping pseudotachylite outcrop is situated within the Tachoshui gneiss, a ~87 Ma granitic body which is related to the Yanshanian igneous activity in South China (Yui et al., 2009;

Figure 1B). The metagranite is composed mainly of quartz, plagioclase, biotite, muscovite, with minor epidote, garnet, chlorite, K-feldspar, apatite, zircon, and iron sulfide. Greenschist facies metamorphism took place during the Neogene orogeny producing a faint gneissic texture, which becomes mylonitic towards the peripheries, and marks the thrust contacts with other rock units. The mylonitic gneiss hosting the pseudotachylite is porphyroblastic with a foliation striking NE to E-W and dipping moderately to the north. Ductile mylonitization was active from 4.14 ± 0.02 to 2.99 ± 0.02 Ma constrained by $^{40}Ar/^{39}Ar$ growth ages from syn-kinematic biotites (Wang et al., 1998), indicating that mylonitic reverse shearing extended into the earlier stages of retrograde exhumation (Wang et al., 1998).

The Hoping pseudotachylite occurs as dark aphanitic veins striking SE and dipping gently to SW in indurated cataclasite within the mylonitic gneiss (Chu et al., 2012). Rheological evolution from ductile to brittle during exhumation was observed in the field and petrographically: cataclasite cross-cuts the mylonitic fabric and was cut by the pseudotachylite laden with down-dipping slickenside-like brushlines (Ferre et al., 2016a). Fault pseudotachylite veins truncate the mylonitic foliation and are sub-millimeter to 1 cm thick, and some connected injection veins concordant with foliation were also found. Contacts between the pseudotachylite vein and the wall rock are sharp, characteristic of brittle frictional deformation. Flow structures and devitrifed microcrystallite formation evidencing melt generation were documented in SEM images, and ultracataclasite with brecciated material of grain size smaller than 10 μm is involved and dispersed throughout the pseudotachylite (Kuo, 2016; Figure 2). Geochemical analysis revealed that the pseudotachylite was generated from very limited melting of mostly biotite content in the mylonite host (Kuo, 2016). Biotite breakdown and associated mineralogy imply that the melt formation temperature was higher than 750°C (Chu et al., 2012; Kuo, 2016). Pure K-feldspar veinlets occasionally penetrating portions of the fault veins revealed fluid infiltration at or immediately after faulting at depths greater than 5 km (Chu et al., 2012).

1.2 | *In-situ* $^{40}Ar/^{39}Ar$ laser microprobe dating analysis

In order to date the Hoping pseudotachylite, a ~2 mm thick section with ~1 cm^2 cross-sectional area was cut perpendicular to a fault vein without K-feldspar veinlets (Figure 2 inset), polished and rinsed before SEM imaging and neutron irradiation as described in Chen, Chan, Lo, and Lu (2016) for *in-situ* $^{40}Ar/^{39}Ar$ laser microprobe dating. Details of the methodology are given in the Supplementary section. In total 40 analyses were performed on the sampled pseudotachylite vein (Figure 2) by laser ablation which produced craters ~50 μm wide and up to ~50 μm deep. The results are listed in Table S1 and presented in Figure 2. The errors of each analysis fall from 0.2 to 1.1 Ma with most being less than 0.7 Ma. The age results are spread between 1.6 and 3.2 Ma with a weighted mean age of 2.58 ± 0.07 Ma. The temporal scatter of the results is generally normally distributed, and slightly bimodal with sub-peaks at ~2 and ~3 Ma (Figure 3 inset). There is no systematic variation in age along- and perpendicular to the vein direction, while the younger ages are more common in finer-grained portions of the analyzed pseudotachylite vein (Figure 2). The acquired ages from the pseudotachylite are mostly younger than the biotite $^{40}Ar/^{39}Ar$ ages obtained from the wall rock mylonite (Wang et al., 1998; Figure 3 inset).

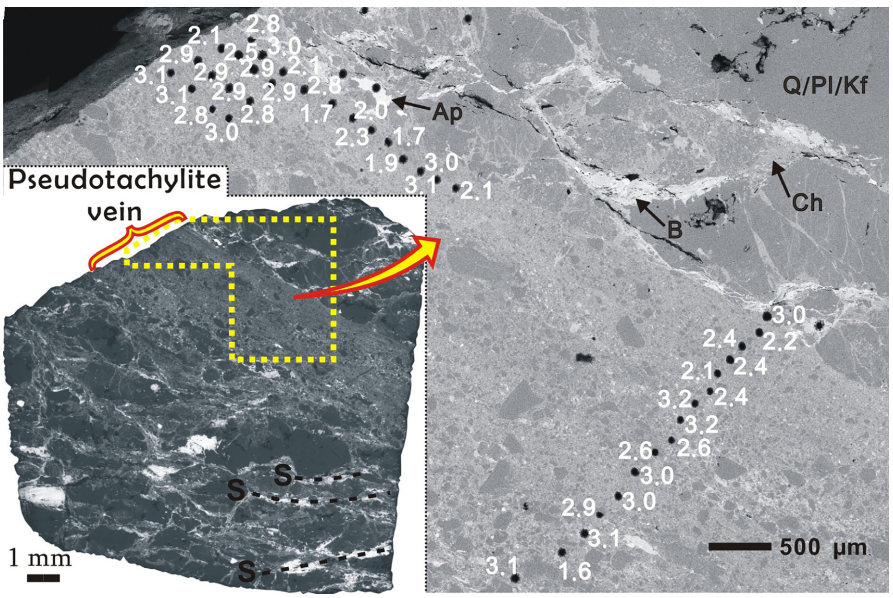

FIGURE 2 SEM backscatter image of the dated pseudotachylite sample (the entire wafer shown in the inset) illustrating detailed melt-cataclasis distribution within the pseudotachylite, with marked *in-situ* $^{40}Ar/^{39}Ar$ laser microprobe dating results. Q, quartz; Pl, plagioclase; Kf, K-feldspar; B, biotite; Ch, chlorite; Ap, apatite. S, general mylonitic foliation in the wall rock [Colour figure can be viewed at wileyonlinelibrary.com]

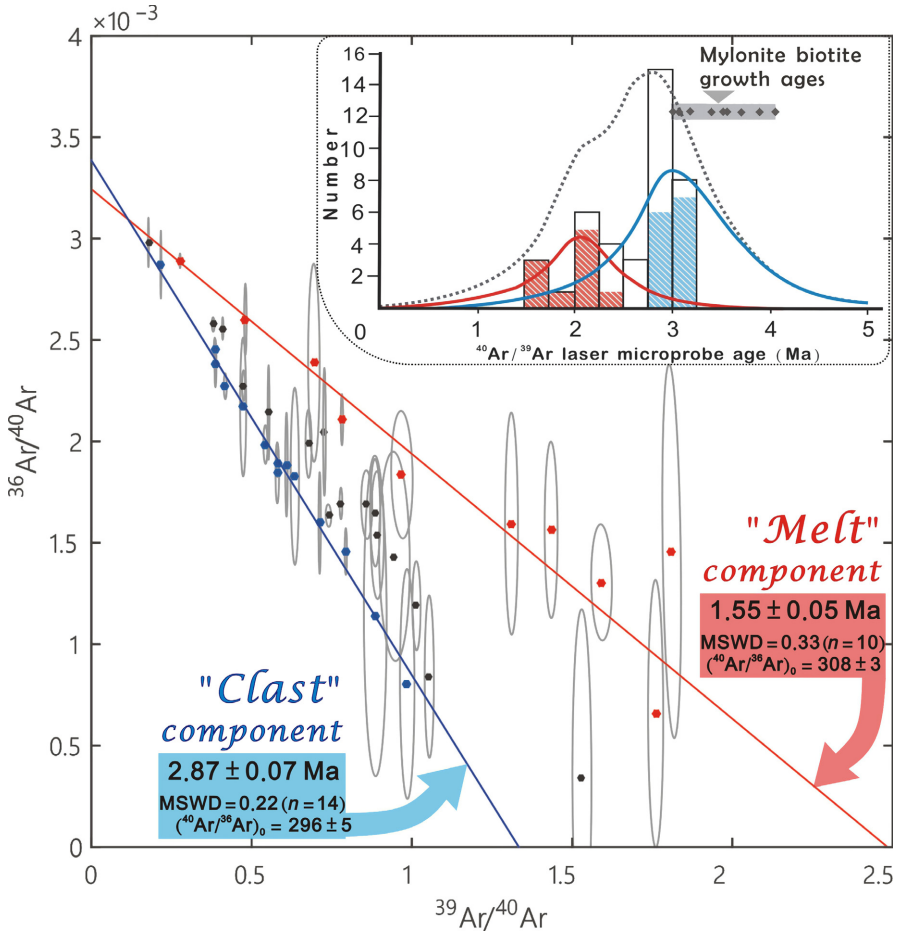

FIGURE 3 Inverse isochron plot for the *in-situ* $^{40}Ar/^{39}Ar$ laser microprobe dating results. Individual data points are presented by solid dots with ± 1σ ellipses, and color coded showing two radiogenic system components. Inset exhibiting histogram of the $^{40}Ar/^{39}Ar$ laser microprobe dating results, with host rock mylonite biotite ages (from Wang et al., 1998) indicated [Colour figure can be viewed at wileyonlinelibrary.com]

1.3 | Timing of pseudotachylite formation

The acquired ages of the Hoping pseudotachylite fall within the latter half of the Taiwan orogeny (Lin et al., 2003), and are generally younger than the biotite in the mylonite host (3.0 to 4.1 Ma; Wang et al., 1998) although the pseudotachylite was mostly derived from biotite melt (Kuo, 2016). The minimum temperature of 750°C for pseudotachylite generation, as inferred from petrographical observations (Chu et al., 2012; Kuo, 2016), is considered sufficient to degas preexisting $^{40}Ar^*$ (Sherlock et al., 2009). Post-faulting thermal resetting of pseudotachylite $^{40}Ar/^{39}Ar$ ages is ruled out since it would require over 10 Ma residence at 220°C for biotite microlites (Sherlock, Watts, Holdsworth, & Roberts, 2004), while the regional thermal history in this period was characterized by rapid cooling during fast exhumation (Hsu et al., 2016) without magmatic or prograde metamorphic effects causing significant Ar loss. Therefore the results correspond to brittle faulting events experienced by the deeply-exhumed metagranite body and the basement complex during the retrograde path (Chu et al., 2012). A straightforward approach would regard the weighted mean age of the results, ~2.6 Ma, as representing the record of a major faulting event from a statistical viewpoint; taking into account the time span of the age results and especially the petrographic characteristics of the Hoping pseudotachylite, however, such simplification is obviously inaccurate and requires further examination.

The temporal dispersion of the ages, though not wide from the analytical point of view, occupies a significant portion of the orogeny evolution. One possible contributing factor is the presence of multiple micro-faults that are being dated. The exact fault surface that slipped and produced melt during each earthquake can be extremely thin in thickness (e.g. Boullier et al., 2009), suggesting that each of the obtained ages might have recorded different earthquakes in the 1.6-3.2 Ma time span as the K-Ar isotopic system at each analyzed site closed since post-melting quench and remained undisturbed. This scenario is regarded as highly unlikely because neither lateral trend of age variations across-vein (e.g. Sherlock et al., 2009) nor textural evidence (Chu et al., 2012; Kuo, 2016) are observed witnessing preservation of multiple fault-parallel principal slip zones thicker than ~ 50 μm (Figure 2).

Taking into account of the textural complexity of the Hoping pseudotachylite, whose melt portion was estimated to be rather low (Kuo, 2016), the analyzed volume of each laser fusion experiment

was prone to contain minute brecciated material whose K-Ar isotopic systems would not be completely reset during earthquake-melting. Such inherited Ar from micro-clasts contaminates the laser microprobe ages whose extent depends on the ratio of non-melt portions within the analyzed volume, and is inevitable since the finer breccia is much smaller (<10 μm) than the diameter of laser ablation pits (~ 50 μm). The unavoidable incorporation of inherited Ar during laser fusion leads to increases in age, from which the youngest acquired ages (1.6-1.7 Ma; Figure 3 inset) can be inferred to represent the maximum age for pseudotachylite formation. A similar situation has been described for pseudotachylites from central-western Carpathian (Kohút & Sherlock, 2003).

Further scrutinized in an inverse isochron plot (Figure 3), the Hoping pseudotachylite results are spread between two end-member inverse isochrons with ages of 2.87 Ma and 1.55 Ma. The inverse isochron plot shows that excess Ar is not apparent since both end-members contain non-radiogenic Ar components with $^{40}Ar/^{36}Ar$ values (295 ± 4 and 308 ± 3) close to atmospheric composition (298.65; Lee et al., 2006). Therefore the laser microprobe results come from various combinations of the non-radiogenic atmospheric source and the two radiogenic sources delineated in the inverse isochron plot (Figure 3). The older 2.87 Ma component may represent, albeit not exactly, the age range of wall rock mylonitic newly grown biotite (Wang et al., 1998), and may be treated as the relic wall rock Ar isotopic system preserved in micro-breccia. The younger inverse isochron of 1.55 Ma may be considered as an isotopic component from the melt portions of the pseudotachylite vein. The younger component deduced from inverse isochron analysis, 1.55 Ma, slightly later than the 1.6-1.7 Ma maximum age inferred from the youngest results, would best represent the age of the pseudotachylite.

1.4 | Seismotectonic implications

The new age constraints from *in-situ* $^{40}Ar/^{39}Ar$ laser microprobe dating results may pinpoint the depth of pseudotachylite formation by incorporating exhumation rates derived from thermochronological documentations. Estimates of this at the retro side of the Taiwanese orogenic wedge (i.e. eastern Central Range) mostly fall between 3 and 6 mm/yr (Fuller et al., 2006), and a recent intensive effort in the northern part of the region yielded a 3 km/Ma exhumation rate since ~1.5 Ma (Hsu et al., 2016). Assuming 1.55 Ma as the age of the seismic event generating the Hoping pseudotachylite, the depth estimate is ~5 km to ~10 km by adopting exhumation rate at 3 and 6 mm/yr, respectively. This estimation agrees well with petrological assessment (Chu et al., 2012). The Hoping pseudotachylite was therefore formed in the shallow portion of the seismogenic zone under the Central Range, demonstrating that seismic faulting is an integral part of rock exhumation in the Taiwanese Central Range.

Given the fast regional rock uplift, the stress state and related parameters of the paleoearthquake(s) fossilized as the Hoping pseudotachylite could reflect what is happening today. Modern seismicity at 5-10 km depth beneath the Central Range is dominated by normal-faulting focal mechanisms (Wu et al., 2008) and interpreted to be due to accelerated exhumation (Lin, 2002) and the lithospheric plate configuration and kinematics (Wu, Kuo-Chen, & McIntosh, 2014). Based on regional brittle structure analysis (Crespi, Chan, & Swaim, 1996), the shallow crust beneath the Central Range, as well as the later parts of rock exhumation within the Taiwanese hinterland, are prevalently extensional. Structural analysis of the Hoping pseudotachylite outcrop suggests that the causative fault was a normal fault (Korren et al., 2017). Therefore the pseudotachylite stands as a record of the tectonic and seismic processes that have operated in the early stages of rock exhumation in the Taiwanese hinterland, and may be viewed as equivalent to present-day hypocentral processes below the Central Range.

ACKNOWLEDGEMENT

We have benefited from insightful discussions with Yu-Chang Chan, Yu-Min Chou, Jyr-Ching Hu, Chia-Yu Lu, En-Chao Yeh, and Jian-Cheng Lee, and language polishing by Jacob Shing-tsu Chu. Constructive comments from Editor Klaus Mezger, Associate Editor, and two anonymous Reviewers are deeply appreciated. This work is financially supported by Ministry of Science and Technology, Taiwan, R.O.C., under grant numbers: 106-2119-M-008-023 (C.-T. Chen), 105-2811-M-002-123 and 106-2116-M-002-017 (C.-H. Lo), and National Central University grants to C.-T. Chen. This is Institute of Earth Sciences, Academia Sinica Contribution No. IESAS2230

ORCID

Chih-Tung Chen http://orcid.org/0000-0002-4498-5513

REFERENCES

Beyssac, O., Simoes, M., Avouac, J.-P., Farley, K.A., Chen, Y.-G., Chan, Y.-C., & Goffe, B. (2007). Late Cenozoic metamorphic evolution and exhumation of Taiwan. *Tectonics*, *26*, TC6001.

Boullier, A.-M., Yeh, E.-C., Boutareaud, S., Song, S.-R., & Tsai, C.-H. (2009). Microscale anatomy of the 1999 Chi-Chi earthquake fault zone. *Geochemistry, Geophysics, Geosystems*, *10*, Q013016.

Chan, Y.-C., Okamoto, K., Yui, T.-F., Iizuka, Y., & Chu, H.-T. (2005). Fossil fluid reservoir beneath a duplex fault structure within the Central Range of Taiwan: Implications for fluid leakage and lubrication during earthquake rupturing process. *Terra Nova*, *17*, 493–499.

Chen, C.-T., Chan, Y.-C., Lo, C.-H., & Lu, C.-Y. (2016). Growth of mica porphyroblasts under low-grade metamorphism- a Taiwanese case using in-situ $^{40}Ar/^{39}Ar$ laser microprobe dating. *Journal of Structural Geology*, *92*, 1–11.

Chen, C.-T., Chan, Y.-C., Lu, C.-Y., Simoes, M., & Beyssac, O. (2011). Nappe structure revealed by thermal constraints in the Taiwan metamorphic belt. *Terra Nova*, *23*, 85–91.

Chiao, C. H. (1991). *The Geologic Structure and Evolution of the Hoping Area in Eastern Taiwan*. Unpubl. m.s. thesis, National Taiwan University, Taipei, Taiwan, R.O.C.

Chu, H.-T., Hwang, S.-L., Shen, P., & Yui, T.-F. (2012). Pseudotachylyte in the Tananao Metamorphic Complex, Taiwan: Occurrence and dynamic phase changes of fossil earthquakes. *Tectonophysics*, *581*, 62–75.

Cowan, D. S. (1999). Do faults preserve a record of seismic slip? A field geologist's opinion. *Journal of Structural Geology*, *21*, 995–1001.

Crespi, J. M., Chan, Y.-C., & Swaim, M. S. (1996). Synorogenic extension and exhumation of the Taiwan hinterland. *Geology*, *24*, 247–250.

Di Toro, G., Nielsen, S., & Pennacchioni, G. (2005). Earthquake rupture dynamics frozen in exhumed ancient faults. *Nature*, *436*, 1009–1012.

Ferre, E. C., Chou, Y.-M., Kuo, R.-L., Yeh, E.-C., Leibovitz, N. R., Meado, A. L., … Geissman, J. W. (2016a). Deciphering viscous flow of frictional melts with the mini-AMS method. *Journal of Structural Geology*, *90*, 15–26.

Ferre, E. C., Yeh, E.-C., Chou, Y.-M., Kuo, R.-L., Chu, H.-T., & Korren, C. S. (2016b). Brushlines in fault pseudotachylytes: A new criterion for coseismic slip direction. *Geology*, *44*, 395–398.

Fuller, C. W., Willett, S. D., Fisher, D., & Lu, C.-Y. (2006). A thermomechnical wedge model of Taiwan constrained by fission-track thermochronometry. *Tectonophysics*, *425*, 1–24.

Hsu, W.-H., Byrne, T. B., Ouimet, W., Lee, Y.-H., Chen, Y.-G., van Soest, M., & Hodges, K. (2016). Pleistocene onset of rapid, punctuated exhumation in the eastern Central Range of the Taiwan orogenic belt. *Geology*, *44*, 719–722.

Kelley, S. P., Reddy, S. M., & Maddock, R. (1994). Laser-probe $^{40}Ar/^{39}Ar$ investigation of a pseudotachylyte and its host rock from the Outer Isles thrust, Scotland. *Geology*, *22*, 443–446.

Kohút, M., & Sherlock, S. C. (2003). Laser microprobe $^{40}Ar/^{39}Ar$ analysis of pseudotachylyte and host-rocks from the Tatra Mountains, Slovakia: Evidence for late Palaeogene seismic/tectonic activity. *Terra Nova*, *15*, 417–424.

Korren, C. S., Ferre, E. C., Yeh, E.-C., Chou, Y.-M., & Chu, H. T. (2017). Seismic rupture parameters deduced from a Pliocene-Pleistocene fault pseudotachylyte in Taiwan. In M. Y. Thomas, T. M. Mitchell & H. S. Bhat (Eds.), *Fault Zone Dynamic Processes: Evolution of Fault Zone Properties and Dynamic Processes During Seismic Rupture AGU Monograph*, (p. 227). Washington, USA: American Geophysical Union.

Kuo, R.-L. (2016). Microstructural and Magnetic Investigations of Pseudotachylyte and Ultracataclasite in the Hoping River, Tananao Complex, Eastern Taiwan. Unpubl. m.s. thesis, National Taiwan University, Taipei, Taiwan, R.O.C.

Lee, J.-Y., Marti, K., Severinghaus, J. P., Kawamura, K., Yoo, H.-S., Lee, J.-B., & Kim, J. S. (2006). A redetermination of the isotopic abundances of atmospheric Ar. *Geochimica Et Cosmochimica Acta*, *70*, 4507–4512.

Lin, C.-H. (2002). Active continental subduction and crustal exhumation: The Taiwan orogeny. *Terra Nova*, *14*, 281–287.

Lin, A. T., Watts, A. B., & Hesselbo, S. P. (2003). Cenozoic stratigraphy and subsidence history of the South China Sea margin in the Taiwan region. *Basin Research*, *15*, 453–478.

Lo, C.-H., & Onstott, T. C. (1995). Rejuvenation of K-Ar systems for minerals in the Taiwan Mountain Belt. *Earth and Planetary Science Letters*, *131*, 71–98.

Sherlock, S. C., Strachan, R. A., & Jones, K. A. (2009). High spatial resolution $^{40}Ar/^{39}Ar$ dating of pseudotachylites: Geochronological evidence for multiple phases of faulting within basement gneisses of the Outer Hebrides (UK). *Journal of the Geological Society (London)*, *166*, 1049–1059.

Sherlock, S. C., Watts, L. M., Holdsworth, R. E., & Roberts, D. (2004). Dating fault reactivation by Ar/Ar laserprobe: And alternative view of apparently cogenetic mylonite-pseudotachylyte assemblages. *Journal of the Geological Society (London)*, *161*, 335–338.

Shyu, J. B. H., Sieh, K., & Chen, Y.-G. (2005). Tandem suturing and disarticulation of the Taiwan orogen revealed by its neotectonic elements. *Earth and Planetary Science Letters*, *233*, 167–177.

Sibson, R. H., & Toy, V. G. (2007). The habitat of fault-generated pseudotachylyte: Presence vs. absence of friction-melt. Earthquakes: Radiated energy and the physics of faulting. *Geophysical Monograph Series*, *170*, 153–166.

Suppe, J. (1981). Mechanics of mountain building and metamorphism in Taiwan. *Memoir of the Geological Society of China*, *4*, 67–89.

Wang, P.-L., Lin, L.-H., & Lo, C.-H. (1998). $^{40}Ar/^{39}Ar$ dating of mylonitization in the Tananao Schist, eastern Taiwan. *Journal of the Geological Society of China*, *41*, 159–184.

Wu, Y.-M., Chang, C.-H., Zhao, L., Teng, T.-L., & Nakamura, M. (2008). A comprehensive relocation of earthquakes in Taiwan from 1991 to 2005. *Bulletin of the Seismological Society of America*, *98*, 1471–1481.

Wu, F. T., Kuo-Chen, H., & McIntosh, K. D. (2014). Subsurface imagine, TAIGER experiments and tectonic models of Taiwan. *Journal of Asian Earth Sciences*, *90*, 173–208.

Yui, T.-F., Okamoto, K., Usuki, T., Lan, C.-Y., Chu, H.-T., & Liou, J.-G. (2009). Late Triassic-Late Cretaceous accretion/subduction in Taiwan region along the east margin of South China - evidence from zircon SHRIMP dating. *International Geology Review*, *51*, 304–328.

SUPPORTING INFORMATION

Additional Supporting Information may be found online in the supporting information tab for this article.

Figure S1. $^{40}Ar/^{39}Ar$ laser microprobe dating sites on hoping pseudotachylite sample with analytical # marked. The analyses which are included in either isochrones in Figure 3 are underlined by blue and red, respectively.Figure S2. Variation in $^{37}Ar/^{39}Ar$ ratio to the age results.Figure S3. Variation in $^{38}Ar/^{39}Ar$ ratio to the age results.Table S1. Results of *in-situ* $^{40}Ar/^{39}Ar$ laser microprobe dating.

How to cite this article: Chen C-T, Wu C-Y, Lo C-H, Chu H-T, Yui T-F. Dating palaeo-seismic faulting in the Taiwan Mountain Belt. *Terra Nova*. 2018;30:146–151.
https://doi.org/10.1111/ter.12319